AD-A068 798 COLUMBIA UNIV DOBBS FERRY NY HUDSON LABS F/G 17/8
THE PANCHROMATIC PRINCIPLE IN OPTICAL FILTERING.(U)
JAN 63 R E WILLIAMS NONR-266(84)
UNCLASSIFIED TM-68 NL

| OF |
AD A068798

END
DATE FILMED
7-79
DDC

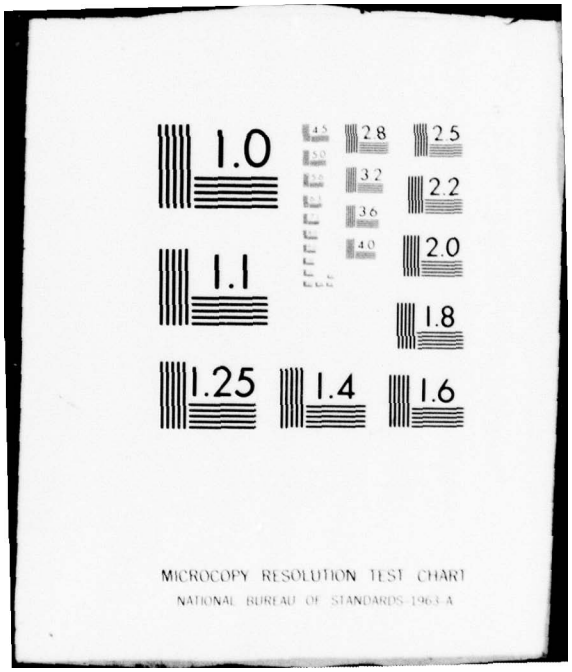
1.0
1.1
1.25
1.4
1.6
1.8
2.0
2.2
2.5
2.8
3.2
3.6
4.0
4.5
5.0
MICROCOPY RESOLUTION TEST CHART
NATIONAL BUREAU OF STANDARDS-1963-A

COPY 2

Hudson Laboratories
of
Columbia University
Dobbs Ferry, New York

(1)

Robert A. Frosch
Director

(9) Technical Memorandum No. 68

(14) TM-68

(6) THE PANCHROMATIC PRINCIPLE IN OPTICAL FILTERING

by

(10) Ross E. Williams

(12) 38 P.

(11) January 30, 1963

UNCLASSIFIED

(15) Nonr-266(84)

This work was supported by the Office of Naval Research.
Reproduction in whole or in part is permitted for any purpose of the United States government.

172 050

[redacted]

MAY 1 1963

A strong need exists in active search and surveillance systems for simultaneous multichannel signal processing capability. The data acquisition rate and its processing in real time have already strained the capacity of conventional search systems, and in some cases an answer is being sought in the duplication and parallel operation of complex equipments. This trend, although dictated under certain circumstances, is undesirable from the standpoint of economic and reliability factors obviously, but also it suffers from limited capability to evolve into more flexible concepts in the near future. Fortunately a number of signal processing techniques have been proposed in recent years, and some of them have been implemented with reasonable success.

The panchromatic optical correlator is one attempt at satisfying a particular requirement of high data rate receivers matched to the transmitted waveform. The technique is presently still in a breadboard stage and its applicability is not fully proven as yet, but it offers a reasonably promising expectation for the simultaneous processing of variously Doppler-distorted signals. This simultaneous approach would obviate the need for a sequential scan of all the Doppler possibilities, which customarily is multiplexed with a real-time correlation process. The technique is particularly applicable in low Q, wide-bandwidth systems in which Doppler distortions cannot be approximated by simple frequency shifts of the signal components. Instead the true scale factor relationship must be maintained between frequency components of the transmitted and received signals:

$$\omega_r = \omega\left(1 \pm \frac{2v}{c}\right) = a\omega \qquad (1)$$

where v = target radial speed, assumed constant for signal duration T,

c = signal propagation speed,

a = Doppler distortion factor,

ω = any particular radian frequency of the transmitted signal, and

ω_r = corresponding radian frequency of the received signal.

An ideal correlation receiver would cross correlate the received signal not only against a replica of the transmitted waveform but against the entire range of all possible Doppler distorted versions of this replica (as dictated by a likely range of v values in Eq. [1]). Such a procedure becomes prohibitively expensive when waveforms of long duration T are used to obtain increased processing gain. A safe criterion for avoiding significant degradation in the correlation process due to timebase contractions or expansions of the type represented by Eq. (1) is the one which states that timebase errors between the received signal waveform and the reference function with which it is correlated shall not accumulate over the signal duration by more than one-quarter period of the highest frequency contributing significant energy to the power spectrum of the signal. For large T, the result is a fantastically large requirement on the number of distinguishable Doppler channels that must be processed simultaneously to cover all possible target motions. A coarser spacing of Doppler channels leads not so much to a lower resolution on target velocity determination as to an outright failure to detect the target. Therefore, the entire range of Doppler distorted signals must be scanned with a resolution which is proportional to the signal duration T. Electronic techniques can be used to time compress the original received

signals and scan the entire Doppler range while processing the received signals in real time. However, such techniques are not generally well adapted to multichannel inputs, as from many receptors. If time-compression is used to permit a scan of Doppler distortions, it is not then available to allow a multiplexing of various received signals onto a single timebase so that a single electronic correlator can perform the receiver-multiplexed correlation. Moreover, the number of received signals to be cross correlated frequently is great enough to require multiple correlation channels if real-time operation is necessary. In such cases, optical correlators have an obvious appeal in their ability to correlate a large number of channels simultaneously without duplication of equipment. The panchromatic optical correlator takes the further step of simultaneous processing all Doppler distortions while maintaining the multiple channel capability at the input.

The principles of coherent optical correlators are well described in the literature.[1] Basically an optical correlator consists of one of several configurations of lenses and apertures which perform the following generalized two-dimensional averaging process (with the exception of the Optical Matched Filter, shown in Fig. 2):

$$H(\omega_x, \omega_y) = \iint_A f(x,y)\, g(x,y)\, e^{j(\omega_x x + \omega_y y)}\, dxdy \qquad (2)$$

---

[1] L. J. Cutrona, E. N. Leith, C. J. Palermo, and L. J. Porcello, "Optical data processing and filtering systems," IRE, Vol. IT-6, No. 3 (June 1960).

The relation among coordinates of Eq. (2) is shown in Fig. 1, and the subscript A indicates integration over the optical aperture. The weighted averaging, in which the kernel $e^{j(\omega_x x + \omega_y y)}$ appears, is a property of optical systems that has been known for some time.[2] Physically the kernel represents the phase of the light amplitude vector at the point (ω_x, ω_y) determined by Huygen's principle from the light amplitude at point (x,y), and the integration represents a coherent summing of light amplitudes over the extent of one of the aperture planes perpendicular to the optic axis. In particular, various restrictions and special conditions upon Eq. (2), which can be simulated by lenses and apertures, can reduce the general expression of Eq. (2) to many of the commonly useful transforms, including Fourier and Laplace transforms, correlations, convolutions, power spectra, ambiguity functions, etc. In addition, with the use of cylindrical lenses it is possible to reduce the two-dimensional integration of Eq. (2) to a one-dimensional one, in which case the unused dimension contains a large number of independent information channels which can be processed simultaneously.

A particularly useful configuration for performing optical correlations has been described previously[1] and is shown schematically in Fig. 2. It uses a coherent monochromatic light source to project the Fourier transform $S(\omega_x)$ of the moving signal function $s(x_1 - x_o)$ upon the reference function Fourier transform, $R^*(\omega_x)$, so that the light amplitude distribution transmitted through the frequency plane in which $R^*(\omega_x)$ is inserted is proportional

---

[2] Max Born, Optik (Julius Springer, Berlin, 1933), Sec. 46-47.

to $S(\omega_x)\ R^*(\omega_x)$. An inverse Fourier transform performed by the lens to the right in Fig. 2 produces the desired correlation function $\phi(x_o)$ in the output plane. This optical arrangement is called a matched filter because it uses, in analogy to electronic matched filters, a spatial frequency filter $R^*(\omega_x)$ matched to the signal $s(x_1)$. In this, or other, configurations a different reference function must be inserted for each different Doppler distortion of the received signal. Therefore, to search the entire range of possible target motions, the reference function must be changed continuously and the various correlation functions for the different Dopplers performed sequentially.

The panchromatic optical correlator depends for its operation upon the fact that a Fourier transform relationship exists between the light amplitude distributions in planes located with respect to a lens, as shown in Fig. 2. This relationship has been known for some time, but its practical application to optical correlators first found expression in the conventional and matched filter configurations. It is further exploited in the panchromatic correlator where advantage is taken of the fact that the scale factor connecting the coordinate of a frequency plane and the corresponding spatial frequency depends on the light wavelength:[1]

$$\omega_x = -\frac{2\pi}{\lambda f}\, x_2 \tag{3}$$

where ω_x = radian spatial frequency associated with x_2,

λ = light wavelength,

f = lens focal length, and

x_2 = coordinate defined on Fig. 2.

It is obvious from Eq. (3), by its dependence upon λ, that a continuous range of scale factors connecting ω_x and x_2 can be obtained by varying the color of the light source. In particular, if we define $\omega_x = \omega_r = a\omega$, and relate x_2 to ω, Eq. (3) can be made to simulate Eq. (1), wherein the reflected signal frequency components appear as scale factor distortions of the original signal components. Thus, a slight broadening of the spectral width of the light source color filter, which is made as monochromatic as possible for usual correlator configurations, can simulate in the panchromatic correlator the Doppler distortions imposed upon the signal by reflection from a moving target.

The complete configuration of a panchromatic correlator is shown in Fig. 3. It differs from earlier correlator types by including a broadened spectral width in the light source and filter, a diffraction grating to allow the use of a heterodyned version of the received signal, a single fixed reference function inserted in a frequency plane, and a color separation prism to resolve the various Doppler channels in the output plane. The reference function, or replica of the transmitted signal spectrum, is introduced as a matched filter, i.e., the complex conjugate of the signal Fourier transform is inserted in a frequency plane as a filter which matches, for a given center wavelength λ^o of the light source, the undistorted transmitted signal. Neglecting the effect of the heterodyning operation performed on the received signal in order to conserve bandwidth prior to insertion into the correlator (to be described in the next paragraph), a continuous range of Doppler distortions can be accommodated by the continuous spectrum of light source frequencies without changing the physical format of the reference function. This format is fixed in terms of the x_2 coordinate of Eq. (3), but Eq. (3) shows that a range of

corresponding ω_x, and therefore a, values is available because of the range of λ values present. In this context, the panchromatic correlator can be considered to be a superposition of many coherent, monochromatic correlators with each light source frequency corresponding to a particular Doppler distortion of the transmitted signal. The various light frequencies are separated to resolve Doppler by the prism just to the left of the output plane in Fig. 3.

A panchromatic correlator could be built according to the foregoing description, and presumably it would properly correlate unheterodyned Doppler distorted signals as claimed. However, for any signal function whose spectrum does not extend down to zero cycles it would make inefficient use of the number of resolvable elements, or time-bandwidth product, in the optical aperture. Any optical system with apertures on the optic axis is necessarily a low-pass filter. Hence, better use of the available bandwidth can be made by heterodyning the signal spectrum down toward zero cycles. The heterodyning operation should not transpose the positive frequency spectrum into the negative frequency region, or vice versa, however, for this would lead to overlays of positive and negative frequency components and distortion of the signal. An expression analogous to Eqs. (1) and (3), but also containing the heterodyning operation, would be written:

$$\omega_x \equiv a\omega - \omega_h = -\frac{2\pi}{\lambda f} x_2 - \omega_h \quad , \tag{4}$$

where ω_h = radian frequency shift effected by heterodyning. It is apparent from Eq. (4) that the simple scale factor $\frac{2\pi}{\lambda f}$ relating ω_x and x_2 in Eq. (3) no longer holds in Eq. (4). Thus, the heterodyning operation

appears to eliminate the possibility of simulating Doppler distortions by a spread in the light spectrum. However, by inserting a diffraction grating immediately after the first objective lens of Fig. 3, it is possible to simulate Eq. (4) so that a spread in light frequencies again simulates Doppler distortions when illuminating a heterodyned received signal function, while the bending of the optic axis into the first order image of the diffraction grating produces the constant frequency shift ω_h. For signals heterodyned down near, but not through, zero cycles, the scale factor relation between ω_x and x_2 which depends upon λ, and the bending of the optic axis, also dependent upon λ, just compensate to give a resultant ω_h which is independent of λ. This is easily shown as follows.

Figure 4 shows the bending of the optic axis into the diffraction orders $n = 0, \pm 1$. The usual diffraction equation[3] gives the locations of principal maxima as

$$n\lambda = d \sin \theta \quad , \tag{5}$$

where n = the diffraction order, and

d = slit separation distance on grating.

Also, from Fig. 4,

$$x_h(\lambda) = g \sin \theta_\lambda = \frac{gn\lambda}{d} \quad , \tag{6}$$

---

[3] F. A. Jenkins and H. E. White, Fundamentals of Physical Optics (McGraw-Hill Book Co., Inc., New York, 1937) 1st ed., Chap. 7.

using Eq. (5). Since the coordinates of Fig. 3 are measured with respect to the optic axis before bending, it is necessary to rewrite Eq. (3) in terms of distances measured from the optic axis after bending. It is shown in Appendix I that the relation of Eq. (3) still holds in the first order diffracted image provided coordinates are measured from the diffracted optic axis. Therefore, in terms of the coordinates on Fig. 4,

$$\omega_x \equiv a\omega - \omega_h = - \frac{2\pi}{\lambda f} \left[x_2 - x_h(\lambda) \right] \quad , \tag{7}$$

where $x_h(\lambda)$ is defined on Fig. 4.

Substituting from Eq. (6),

$$\omega_x \equiv a\omega - \omega_h = - \frac{2\pi}{\lambda f} x_2 + \frac{2\pi n g}{fd} \quad . \tag{8}$$

For $n = -1$ in Eq. (8), the term $\frac{2\pi g}{fd}$ represents the constant ω_h, and therefore the frequency shift effected by heterodyning. Then the remainder of Eq. (8) becomes

$$a\omega = - \frac{2\pi}{\lambda f} x_2 \quad ,$$

or

$$x_2 = - \left(\frac{f}{2\pi} \right) a\lambda\omega = \frac{f}{2\pi} \lambda^o \omega \quad . \tag{9}$$

where λ^o is that wavelength corresponding to $a = 1$ (no Doppler distortion). It is now obvious from Eq. (9) that the reference function can be constructed as a function of x_2, which is related to the transmitted (undistorted) signal

frequencies ω by the constant $\left(-\frac{f}{2\pi}\right)\lambda^{o}$. However, the reference function will also represent any other value of a for which

$$a\lambda = \lambda^{o} \quad . \tag{10}$$

The ability of the panchromatic correlator simultaneously to represent all Doppler distortions of the transmitted signal (all a) is illustrated graphically in Fig. 5. Here the Doppler distorted received signal $a\omega$ is plotted horizontally; λ and the Doppler distortion factor a are plotted vertically. The frequency axis for the transmitted spectrum ω is plotted horizontally at $\lambda = \lambda^{o}$ and covers the bandwidth from A to B. For a single transmitted component ω, Eq. (10) gives a hyperbolic relation between a and λ, which is shown in Fig. 5 by the hyperbolic curve connecting A', A and A'', all corresponding to minimum ω (or B', B and B'' for maximum ω). Thus, the horizontal segments $A'B'$, AB, and $A''B''$ represent the received signal spectrum width after negative, zero, and positive Doppler distortions, respectively. The reference function recorded as a function of x_2 for the transmitted signal of spectrum width AB accommodates all distortions of this signal represented by other horizontal segments connecting the two hyperbolic curves of Fig. 5 so long as Eq. (10) holds true. The light source spectrum width is chosen to insure the latter. The constant heterodyning shift $\omega_h = \frac{2\pi g}{fd}$ appears on Fig. 5 as a straight vertical line, independent of λ.

It is apparent from Fig. 4 and Eq. (8) that negative x_2 and n values simulate the Doppler distortion and heterodyning operations that have occurred on the positive ω_x part of the signal spectrum, while positive x_2 and n values do the same for the negative spectrum. Now it is obvious that a matched

filter operation, of the type shown in Fig. 2, can be carried out by inserting the complex conjugate of the transmitted signal positive frequency spectrum in the ω_x plane, centered a distance $-x_h(\lambda^o)$ from the original axis as shown in Fig. 4, and the complex conjugate of the negative spectrum symmetrically displaced a distance $+x_h(\lambda^o)$ from the original axis. Actually only the positive or the negative spectrum need be used, for the omission of either merely causes a light loss by a factor of two in the intensity of the correlation function in the output plane. This result is demonstrated in Appendix II.

In general, the signal spectrum is complex, and, therefore, both amplitude (opacity) and phase (thickness) recordings must be included in the optical version of the reference function inserted in plane $P2_\lambda o$ (Fig. 3). However, there is a large class of signals for which no phase variation is required. These include all signals whose Fourier transforms are purely real or purely imaginary, corresponding to signals which are purely even or purely odd functions of time. The use of such signals considerably simplifies the construction of an optical reference, for only amplitude recording is then necessary.

When the inverse transform is taken by lens L2 of Fig. 3, a sum of superimposed correlation functions, one for each light frequency, will appear in plane P3. A more exact description would note that the optic axis for lens L2 in Fig. 3 cannot be colinear with the diffracted optic axes for all wavelengths. This lack of colinearity has two effects upon the correlation function in plane P3:

1) A slight displacement $\Delta\omega_x(\lambda)$ of diffracted axes, relative to the axis for lens L2 and other components to the right of L2 in Fig. 3, exists at all light wavelengths except for a particular matched wavelength λ^o. This

small displacement is a frequency shift which can be ignored, however, since a displacement $\Delta\omega_x(\lambda)$ in the positive (or negative) frequency plane produces a multiplying phase factor $\exp[-j\Delta\omega_x(\lambda)x_3]$ in the next spatial plane P3, where the correlation function is imaged. Since light intensity, rather than amplitude, is sensed by an output film or photodetector, the absolute square of the correlation coefficient is detected and phase factors of the type $\exp[-j\Delta\omega_x(\lambda)x_3]$ are not apparent.

2) In general, the plane $P2_\lambda$ for a given light frequency is slightly inclined (not exactly perpendicular) to the optic axis of lens L2. Thus, the plane $P2_\lambda o$, which is actually perpendicular to the L2 axis and in which the reference function is inserted, has a light amplitude distribution which, for arbitrary λ, is not quite the Fourier transform of that existing in plane P1, but rather is one which, by reason of the tilted wavefront $P2_\lambda$, can be described by assigning to the Fourier transform a phase shift linear with displacement in the $P2_\lambda o$ plane. Thus, the light amplitude distribution transmitted through $P2_\lambda o$ is of the form $S(\omega_x)\,R^*(\omega_x)\,e^{jk(\lambda)\omega_x}$, where $e^{jk(\lambda)\omega_x}$ is the phase factor and the constant $k(\lambda)$ is a measure of the angle between $P2_\lambda$ and $P2_\lambda o$. The action of lens L2 in performing the inverse Fourier transform converts this phase factor to a time displacement $k(\lambda)$ in plane P3,[4] and this time displacement is dependent upon λ. Thus, the time axis in P3 does not have the same origin for all λ, and the output plane at P4 must be properly calibrated with regard to λ.

[4] P. M. Woodward, Probability and Information Theory with Applications to Radar (McGraw-Hill Book Co., Inc., New York, 1953), table, p. 28

The light intensity available at plane $P2_\lambda$, when illuminated from the on-axis point of plane P1, is given by the usual expression for the light intensity distribution from a plane wavefront impinging on a grating:[3]

$$I = R_o^2 \frac{\sin^2\beta}{\beta^2} \frac{\sin^2 N\gamma}{\sin^2\gamma} , \qquad (11)$$

where $\beta = \frac{\pi a \sin\theta}{\lambda}$,

θ = diffraction angle,

a = grating slit width,

$\gamma = \frac{\pi d \sin\theta}{\lambda}$,

d = grating slit separation, and

N = number of slits in the grating.

By making the slit width a large (e.g., equal to one half the slit separation d), it is possible to narrow the single slit modulating envelope $\frac{\sin^2\beta}{\beta^2}$ so that most of the light is concentrated in the $n = 0, \pm 1$ orders. There is also a requirement that the various diffraction orders do not overlap at plane $P2_\lambda$ and thereby confuse the resulting image. This requirement is met by using long focal length lenses and small slit separation d on the grating to provide a large diffraction angle θ. The joint requirements of light intensity distribution and image separation can be achieved by making $d = 2a$, with d small. It is also possible, on ruled gratings, to taper the bottom of each cut so as to concentrate up to 90 percent of the transmitted light intensity into the first (e.g., $n = -1$) order at the expense of the central ($n = 0$) and higher order images. Phase gratings in which all parts of the grating are equally transparent but differ in optical thickness not only preserve that light normally lost in the opaque regions of conventional gratings, but can

also be constructed to concentrate light in the first order images at the expense of the central image.

The diffraction pattern from grating G1 has secondary maxima at angles close to the primary maxima, and these will add incoherent illumination to the primary maximum diffraction image in plane $P2_\lambda$. It can be shown, however, that the intensity of a particular secondary maximum relative to that of the primary maximum is approximately $4/\pi^2(2n+1)^2$, where n is the number of the secondary maximum counting from the nearest primary maximum. The total intensity received from all secondary maxima within an angular width $\pm\theta_\lambda o/2$, the assumed angular width of the image, to either side of a primary maximum is approximately

$$\frac{8}{\pi^2}\sum_{n=1}^{(N-2)/2}\frac{1}{(2n+1)^2} \doteq .20 \qquad (12)$$

However, the angular width of the principal maximum is twice that of the secondaries. Therefore, the relative noncoherent illumination supplied by the secondary maxima is approximately one half of Eq. (12), or 10 percent of the intensity in the principal maximum. In most cases, the 10-percent increase in noise level will not significantly affect the detectability of a signal which usually is recorded with additive noise of much larger proportions.

It might seem that the angular width of the $n = +1$ or -1 principal maximum would also limit system performance by degrading the inherent

angular resolution. However, it is easily shown* that this is an aperture effect, independent of the grating constants, and so long as the aperture in which the grating is placed is the same size as other apertures of the system, the angular resolution will be the same throughout.

The prism preceding the output plane P4 of Fig. 3 separates the various light colors, or Doppler channels, into a continuous spectrum spread vertically. This vertical spread need not produce any overlap of closely

---

* The angular location of the first minimum to either side of the $n = +1$ principal maximum is given by [3]

$$\sin \theta_{min} = \frac{(N \pm 1)\lambda}{Nd} ,$$

while that of the principal maximum is

$$\sin \theta_{max} = \frac{\lambda}{d} .$$

For large N, the half width $|\theta_{max} - \theta_{min}|$ of the principal maximum is obtained from

$$|\sin \theta_{max} - \sin \theta_{min}| = |d(\sin \theta_{max})| = \cos \theta_{max}\, d\theta_{max}$$

$$= \lambda / Nd$$

$$d\theta_{max} = \lambda / Nd \cos \theta_{max} = \lambda / A ,$$

where A = total aperture. This is the approximate expression for the angular resolution of a circular aperture of diameter A.

spaced signal channels from the signal film (plane P1), for optical magnification between planes P3 and P4 can produce many more resolvable channels on P4 than existed in P1 by enlarging the format. Moreover, the vertical, or y_1, spacing of channels in P1 is dictated by the overall resolution of the correlator as a whole (film plus lens components acting as cascaded filters), whereas the channel spacing in plane P4 need only exceed the resolution distance on the film alone. It should be noted that the optical transformation between planes P3 and P4 is a true imaging process and not a Fourier transform relationship. Put in different terms, the power of lens L3 is such that both the Fourier transform and its inverse are accomplished between P3 and P4.

The prism can also be oriented, as shown in Fig. 6, so as to produce a horizontal, or x, spread of the spectrum. To avoid confusion between the time axis and Doppler channels, it would then be necessary to insert a slit in plane P3 and use the x axis in plane P4 for the Doppler (λ) as well as the time (x_o) coordinate, as shown in Fig. 6. In this configuration the correlation function $\phi(x_o)$ is not simultaneously observable over a wide x_o range, as it is in the configuration of Fig. 3. Instead, only $\phi(x_o)$ for that x_o value corresponding to the slit position is sampled at one instant of time. With the signal film continuously traversing plane P1 in real time, the output through the slit at plane P3 (or its Doppler separated version at P4) provides a time-evolving history of $\phi(x_o)$. To avoid information smear on the output film, the Doppler spread ($\lambda^- \ldots \lambda^+$) must be sampled at P4 in time increments Δx_o, and the Doppler determinations must be multiplexed with the real time x_o variation. This leads naturally to some sort of

frame camera for recording information appearing at P4 , but the resulting multiplexing of Doppler and time, or x_o , information may not be particularly convenient for subsequent data reduction. Moreover, a much shorter exposure time, equal to Δx_o , is available in the configuration of Fig. 6 than in that of Fig. 3, where a plot of $\phi(x_o)$ for a range of x_o values is available at P3 (or P4) and exposes a film moving slowly through the P3 (or P4) plane synchronously with the signal film motion through P1 .

For some purposes the prism can be eliminated entirely and the various Doppler channels left unresolved in plane P4 . The correlator then becomes Doppler invariant, regardless of whether or not the original signal function was chosen to be Doppler invariant. This can be a very convenient mode of operation when one wishes not only to make no use of Doppler information but also needs to insure that Doppler distortions of a target reflected signal do not cause the original signal to decorrelate. Of course, a particular constant velocity target motion will then give rise to a received signal which correlates at only one light frequency, and illumination in the output plane from all other parts of the light spectrum will then appear as noise superimposed on the desired correlation function. Therefore, if the Doppler channels are left unresolved in P4 , the signal-to-noise ratio in plane P1 must be adequate to insure a detection at P4 in the presence of noise from other light frequencies.

Since the distortion of the signal timebase by a scale factor due to moving target reflections, or the distortion of its frequency components by the inverse of this scale factor, is normally a small percentage distortion, the range of light frequencies required for Doppler compensation is a small percentage of the center frequency (see Eq. [1]). Therefore, no compensation need be made for the spectral response of the light source or the film in the

output plane P4 over the narrow spectral range actually used. However, the same usually cannot be said for the band-pass interference filter F1 (Fig. 3), whose frequency response curve has skirts that do not fall to zero infinitely fast at the edges of the pass region. To the extent that compensation must be made, the light intensities in plane P4 may be interpreted after weighting them with the inverse frequency response of the filter F1.

The relative merits of the panchromatic principle can be summarized by reviewing the advantages and disadvantages implied in the foregoing. The advantages relative to other optical correlation techniques appear to include the following:

1) A single reference function for correlation against all Doppler distortions of the signal.
2) Simultaneous correlation of all Doppler distorted signals, rather than a sequential Doppler search multiplexed with real time (or range).
3) No mechanical motions required either for Doppler search or heterodyning.
4) Longer time available to expose film in the output plane P4, by reason of 2), above.
5) Simplicity of parts relative to the number and complexity of operations accommodated (heterodyning, Doppler compensation, correlation).

The principal disadvantage of the panchromatic configuration results from its inefficient use of light flux available at the source. Roughly 90 percent of the initial light flux is lost by retaining only one order (n value) in the

diffraction image produced by simple gratings. Where light source intensity is not a limitation, or where advantage 4), above, compensates, or when special gratings are used to concentrate light in the $n = -1$ order, this is obviously not a problem. In any event, the potential capability of the panchromatic configuration to perform simultaneous Doppler compensation and correlation operations on heterodyned signals appears intriguing and theoretically promising.

ACKNOWLEDGMENTS

The author would like to thank Messrs. Luc Crousel, Howard Schimmel, and Frederik Weindling for their critical review of this manuscript and several helpful suggestions concerning its presentation.

APPENDIX I

The complex light amplitude vector $\hat{E}_2(x_2, y_2)$ at point (x_2, y_2) of plane P2 (see Fig. 7) results from summing the contributions $\hat{E}_1(x_1, y_1)$ from all points (x_1, y_1) of plane P1. Neglecting the obliquity factor and the time dependent factor, this vector sum can be written [1]

$$\hat{E}_2(x_2, y_2) = \iint \hat{E}_1(x_1, y_1)\, e^{-j\frac{2\pi}{\lambda} r(x_1, y_1, x_2, y_2)}\, dx_1\, dy_1 \quad , \qquad (13)$$

where $r(x_1, y_1, x_2, y_2)$ is the optical path length between points (x_1, y_1) in P1 and (x_2, y_2) in P2. When a diffraction grating is present, Eq. (13) can be used to calculate the amplitude vector in any order of the diffraction image, providing r represents the distance to the image point in that order and the various orders are non-overlapping. Figure 7 shows the geometry involved for a particular wavelength and the $n = -1$ (first order) diffracted image. It is apparent from the figure that the optical distance $r_o(x_2)$ from any point of the tilted plane P1′ to x_2 is

$$r_o(x_2) = r_1 + r_2 = g' \cos i + \frac{f}{\cos(\theta - \theta_o)} \quad , \qquad (14)$$

where r_1 is the incident ray and r_2 the diffracted ray to the first order diffracted image. The condition for the first order principal maximum of the diffraction image is

$$d(\sin\theta - \sin i) = \lambda$$

$$\sin i = \sin\theta - \sin\theta_o$$

where $\sin\theta_o = \frac{\lambda}{d}$ and θ_o is the angular position of the principal maximum when $i = o$. Substituting for $\cos i$, Eq. (14) becomes

$$r_o(x_2) = g'\sqrt{1-(\sin\theta - \sin\theta_o)^2} + f\sqrt{1+\tan^2(\theta-\theta_o)}$$

Expanding the trigonometric functions and retaining powers of the angles below the fourth,

$$r_o(x_2) = g'\sqrt{1-\left(\theta - \frac{\theta^3}{6} - \theta_o + \frac{\theta_o^3}{6}\right)^2} + f\sqrt{1+\left[(\theta-\theta_o) + \frac{(\theta-\theta_o)^3}{3}\right]^2}$$

$$\doteq g' + f - \frac{g'}{2}\left[\left(\theta - \frac{\theta^3}{6}\right)^2 - 2\left(\theta - \frac{\theta^3}{6}\right)\left(\theta_o - \frac{\theta_o^3}{6}\right) + \left(\theta_o - \frac{\theta_o^3}{6}\right)^2\right]$$

$$+ \frac{f}{2}\left[(\theta-\theta_o)^2 + \frac{2}{3}(\theta-\theta_o)^4 + \frac{(\theta-\theta_o)^6}{9}\right]$$

$$\doteq g' + f + \frac{1}{2}(f-g')(\theta-\theta_o)^2 \qquad (15)$$

Any other point x_1 of plane P1 will be closer to or further from x_2 than plane P1' by a distance $(-x_1 \sin i)$:

$$
\begin{aligned}
-x_1 \sin i &= -x_1 (\sin\theta - \sin\theta_o) \\
&\doteq -x_1 \left[(\theta - \theta_o) - \frac{(\theta^3 - \theta_o^3)}{6} \right] \doteq -x_1 \left[\tan(\theta - \theta_o) - \frac{\left(\theta^3 - \theta_o^3 - 2\theta^2\theta_o + 2\theta\theta_o^2\right)}{2} \right] \\
&= -x_1 \left[\frac{(x_2 - x_h)}{f} - \frac{\left(\theta^3 - \theta_o^3 - 2\theta^2\theta_o + 2\theta\theta_o^2\right)}{2} \right] \\
&\doteq \frac{-x_1 (x_2 - x_h)}{f} \qquad (16)
\end{aligned}
$$

where the second term on the right side, involving third order differences in θ and θ_o and their products, is neglected.

To justify this neglect, it must be shown that the value of this term is of the same order or smaller than the angular resolution due to the aperture, i.e., the angular width of a principal maximum in the diffraction image, which is given by λ / Nd. It is not hard to choose a set of practical values for N, d, and f which meet this condition while still avoiding an overlap of adjacent orders in the diffraction image.

Adding Eq. (16) to Eq. (15),

$$
r(x_1, x_2) \doteq g' + f + \frac{1}{2} (f - g') (\theta - \theta_o)^2 - \frac{x_1 (x_2 - x_h)}{f} .
$$

Allowing $g' = f$ and neglecting the constant terms g' and f, the remaining term is just $-x_1 (x_2 - x_h)/f$. For two dimensions, the optical distance $r(x_1, y_1, x_2, y_2)$, apart from constant terms, becomes

$$r(x_1, y_1, x_2, y_2) = - \frac{x_1(x_2 - x_h)}{f} - \frac{y_1 y_2}{f} \qquad (17)$$

Equation (13) can now be written

$$\hat{E}_2(x_2, y_2) = \iint \hat{E}_1(x_1, y_1)\, e^{+ j \frac{2\pi}{\lambda f} \left[x_1(x_2 - x_h) + y_1 y_2 \right]} dx_1\, dy_1$$

or

$$\hat{E}_2(\omega_x, \omega_y) = \iint \hat{E}_1(x_1, y_1)\, e^{- j(\omega_x x_1 + \omega_y y_1)} dx_1\, dy_1$$

where $\omega_x \equiv \frac{2\pi}{\lambda f} (x_2 - x_h)$, and

$$\omega_y \equiv - \frac{2\pi}{\lambda f} y_2$$

Since $(x_2 - x_h)$ and y_2 , and therefore ω_x and ω_y , are measured from the diffracted optic axis whose location is a function of λ , they will have different values, when describing a particular point in plane $P2_\lambda$, for the various light wavelengths $\lambda^- \ldots \lambda^+$.

APPENDIX II

The Fourier transform of the delayed received signal $f(t+\tau)$ can be written

$$[N_+(\omega) + kS_+(\omega)]\, e^{j\omega\tau} + \text{complex conjugate} \quad , \tag{18}$$

where

$N_+(\omega)$ = additive noise positive frequency spectrum in the received function f(t),

$S_+(\omega)$ = positive frequency spectrum of the signal s(t),

k = constant $\ll 1$, representing signal amplitude relative to the noise,

$[N_+(\omega) + kS_+(\omega)]$ = positive frequency spectrum of the received function f(t), and

$[N_+(\omega) + kS_+(\omega)]e^{j\omega\tau}$ = positive frequency spectrum of the delayed received function $f(t+\tau)$.

The positive frequency spectrum obtained from Eq. (18) after heterodyning by an amount Ω is

$$[N_+(\omega+\Omega) + kS_+(\omega+\Omega)]e^{j(\omega+\Omega)\tau} \quad ,$$

and this quantity is multiplied by $S_+^*(\omega+\Omega)$ in a matched filter receiver, such as the panchromatic correlator, to form

$$[N_+(\omega+\Omega) + kS_+(\omega+\Omega)]\, e^{j(\omega+\Omega)\tau}\, S_+^*(\omega+\Omega) \quad .$$

The correlation function $\phi_+(t+\tau)$, derived from the positive frequencies only, is found from the inverse Fourier transform of Eq. (18), an operation which is performed by lens L2 in Fig. 3:

$$\phi_+(t+\tau) = \frac{k}{2\pi}\int_0^\infty |S_+(\omega+\Omega)|^2 e^{j(\omega+\Omega)\tau} e^{j\omega\tau} d\omega$$

$$= \frac{k e^{j\Omega\tau}}{2\pi}\int_0^\infty |S_+(\omega+\Omega)|^2 [\cos\omega(t+\tau) + j\sin\omega(t+\tau)] d\omega ,$$

where it is assumed that no correlation exists between the noise and the signal. Letting

$$X(t+\tau) = \frac{k}{2\pi}\int_0^\infty |S_+(\omega+\Omega)|^2 \cos\omega(t+\tau) d\omega$$

and

$$Y(t+\tau) = \frac{k}{2\pi}\int_0^\infty |S_+(\omega+\Omega)|^2 \sin\omega(t+\tau) d\omega ,$$

$$\phi_+(t+\tau) = [X(t+\tau) + jY(t+\tau)] e^{j\Omega\tau}$$

$$= X(t+\tau)\cos\Omega\tau - Y(t+\tau)\sin\Omega\tau + j[Y(t+\tau)\cos\Omega\tau + X(t+\tau)\sin\Omega\tau] .$$

A detector (film, camera tube, etc.) in the output plane of the correlator will be sensitive to light intensities rather than amplitudes, and, therefore, to $|\phi_+(t+\tau)|^2$ rather than $\phi_+(t+\tau)$. Therefore, it will sense

$$|\phi_+(t+\tau)|^2 = [X(t+\tau)]^2 + [Y(t+\tau)]^2$$

However, if both positive and negative frequencies had been retained in the matched filter operation, the correlation function would have been

$$\phi(t+\tau) = \frac{k}{2\pi} \int_0^\infty |S_+(\omega+\Omega)|^2 e^{j(\omega+\Omega)\tau} e^{j\omega\tau} d\omega + \frac{k}{2\pi} \int_{-\infty}^0 |S_-(\omega-\Omega)|^2 e^{j(\omega-\Omega)\tau} e^{j\omega\tau} d\omega$$

But for any real signal s(t)

$$S_+(\omega+\Omega) = S_-^*(-\omega-\Omega)$$

and

$$|S_+(\omega+\Omega)|^2 = |S_-(-\omega-\Omega)|^2$$

Thus,

$$\phi(t+\tau) = \frac{k}{2\pi} \int_0^\infty |S_+(\omega+\Omega)|^2 \left[e^{j(\omega+\Omega)\tau + j\omega t} + e^{-j(\omega+\Omega)\tau - j\omega t} \right] d\omega$$

$$= \frac{k}{\pi} \int_0^\infty |S_+(\omega+\Omega)|^2 [\cos\omega(t+\tau)\cos\Omega\tau - \sin\omega(t+\tau)\sin\Omega\tau]\, d\omega$$

$$= 2[X(t+\tau)\cos\Omega\tau - Y(t+\tau)\sin\Omega\tau]$$

and

$$|\phi(t+\tau)|^2 = 2[X(t+\tau)]^2 + 2[Y(t+\tau)]^2 + 2\{[X(t+\tau)]^2 - [Y(t+\tau)]^2\}\cos 2\Omega\tau$$

$$- X(t+\tau)\, Y(t+\tau) \sin 2\Omega\tau$$

Because the heterodyning frequency shift Ω is generally larger than the signal bandwidth accepted by the optical correlator, such terms as $\cos 2\Omega\tau$ and $\sin 2\Omega\tau$ average to zero within the space covered by one resolvable spot on the output film (or photodetector). Then the light intensity which is actually detected becomes

$$|\phi(t+\tau)|^2 = 2[X(t+\tau)]^2 + 2[Y(t+\tau)]^2 ,$$

just twice the value of $|\phi_+(t+\tau)|^2$. Thus, the net effect of operating only on the positive frequency spectrum of the received function f(t) is one of reducing the available light level at the output by a factor of two. For mechanical convenience the panchromatic correlator is designed to accept only the positive frequency spectrum, thereby generating $|\phi_+(t+\tau)|^2$ at its output.

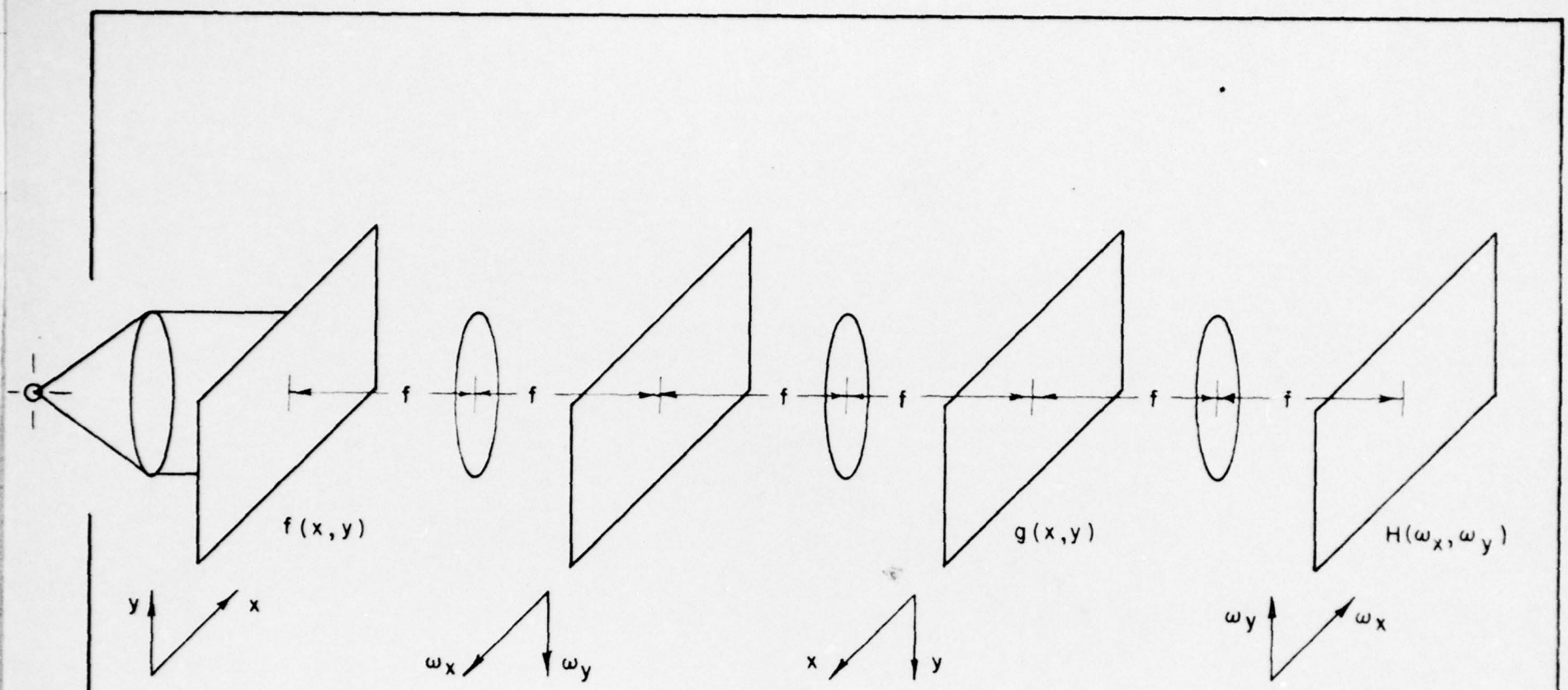

FIGURE 1 OPTICAL FILTER

OPTICAL MATCHED FILTER

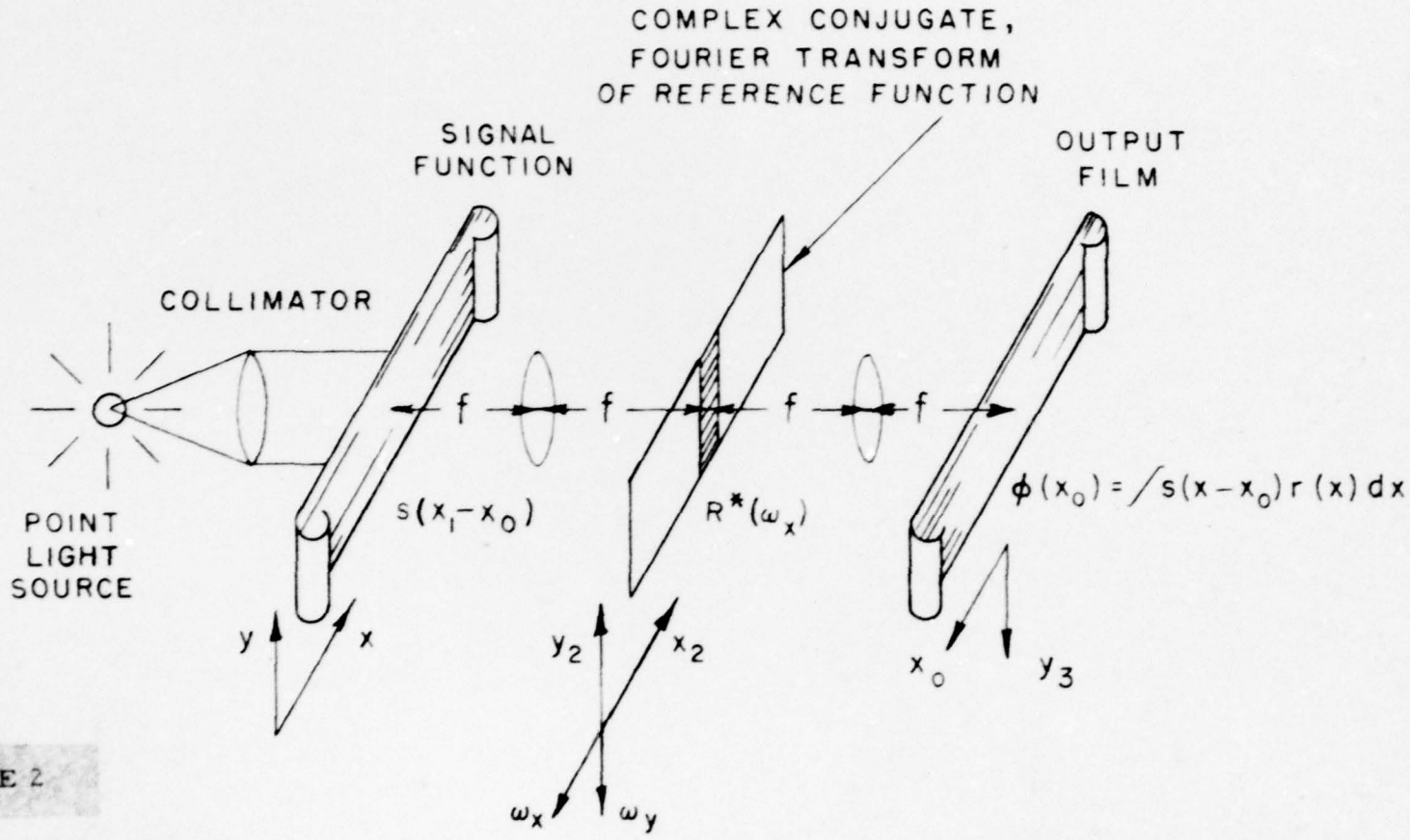

FIGURE 2

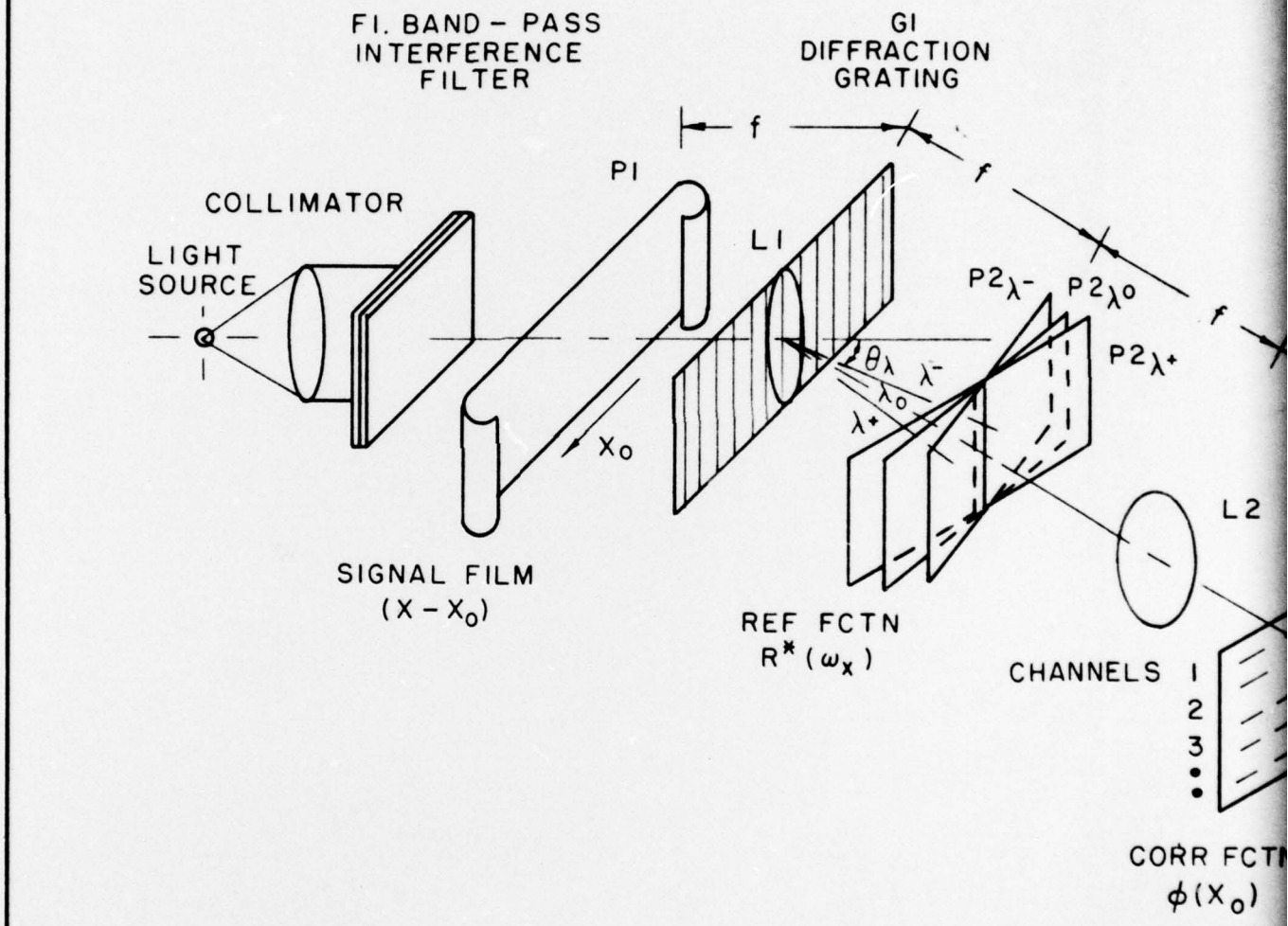

FIGURE 3 PANCHROMATIC CORRELATOR LAY

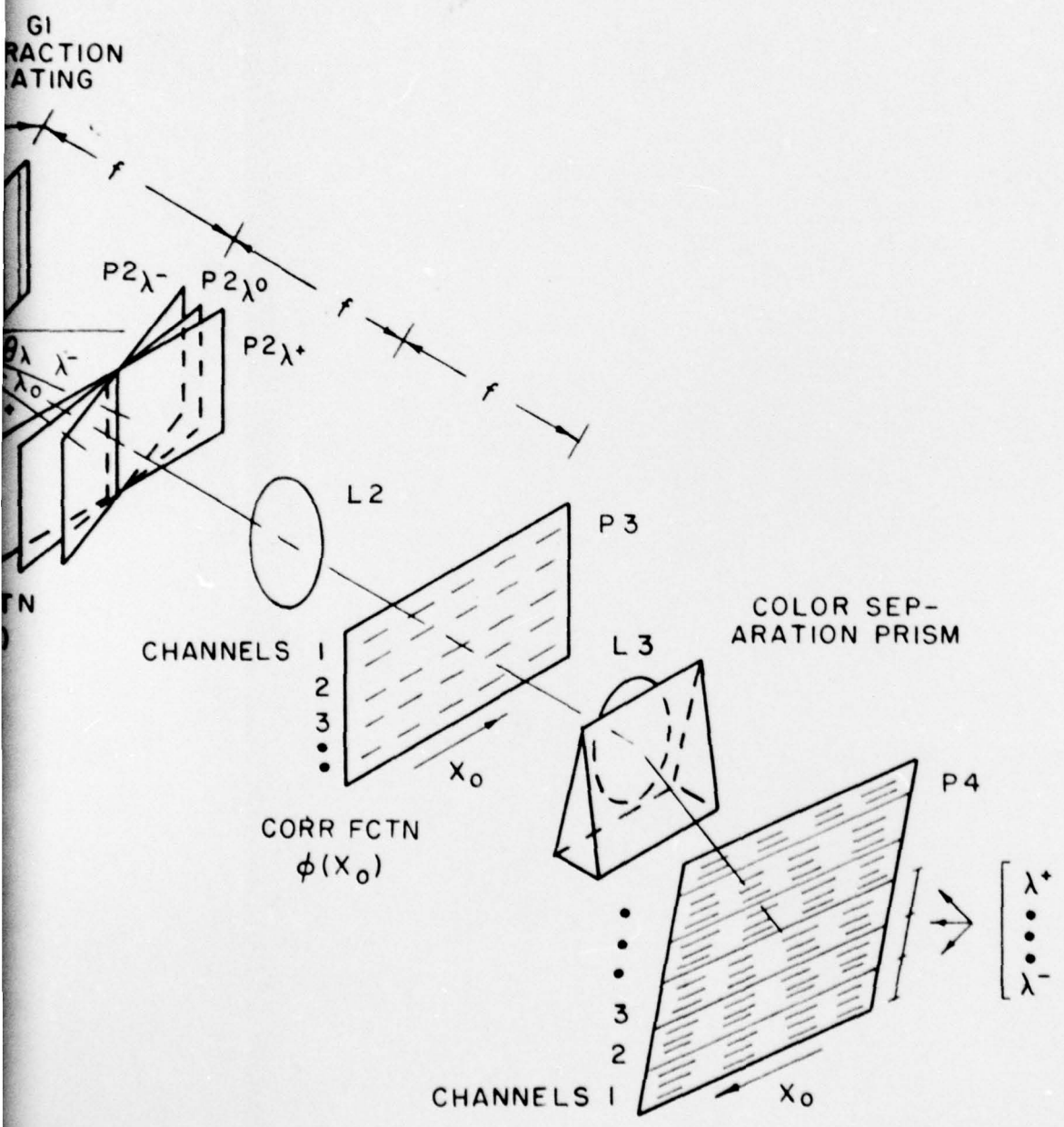

OMATIC CORRELATOR LAYOUT

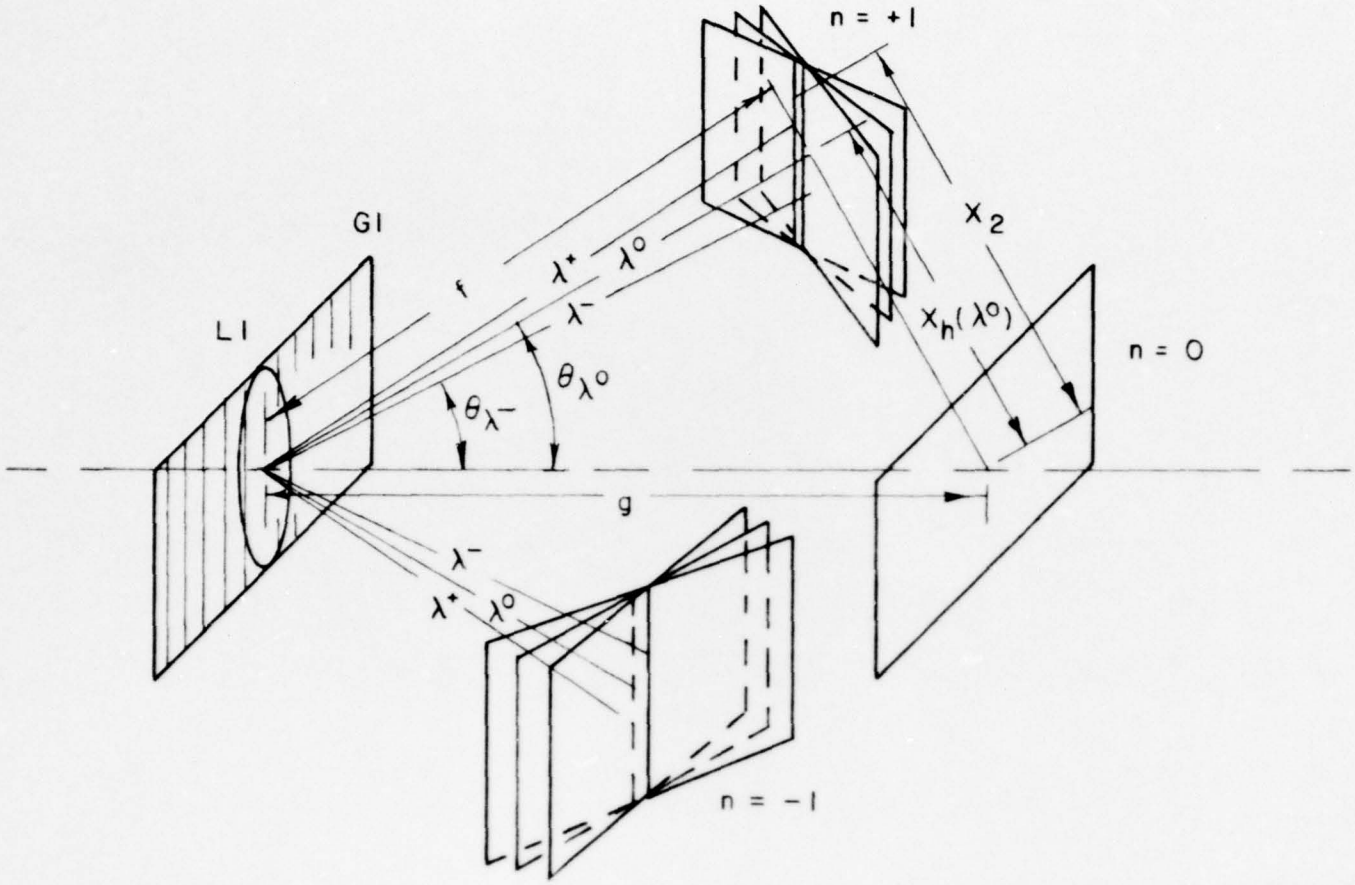

FIGURE 4 DIFFRACTED IMAGE IN PANCHROMATIC CORRELATOR

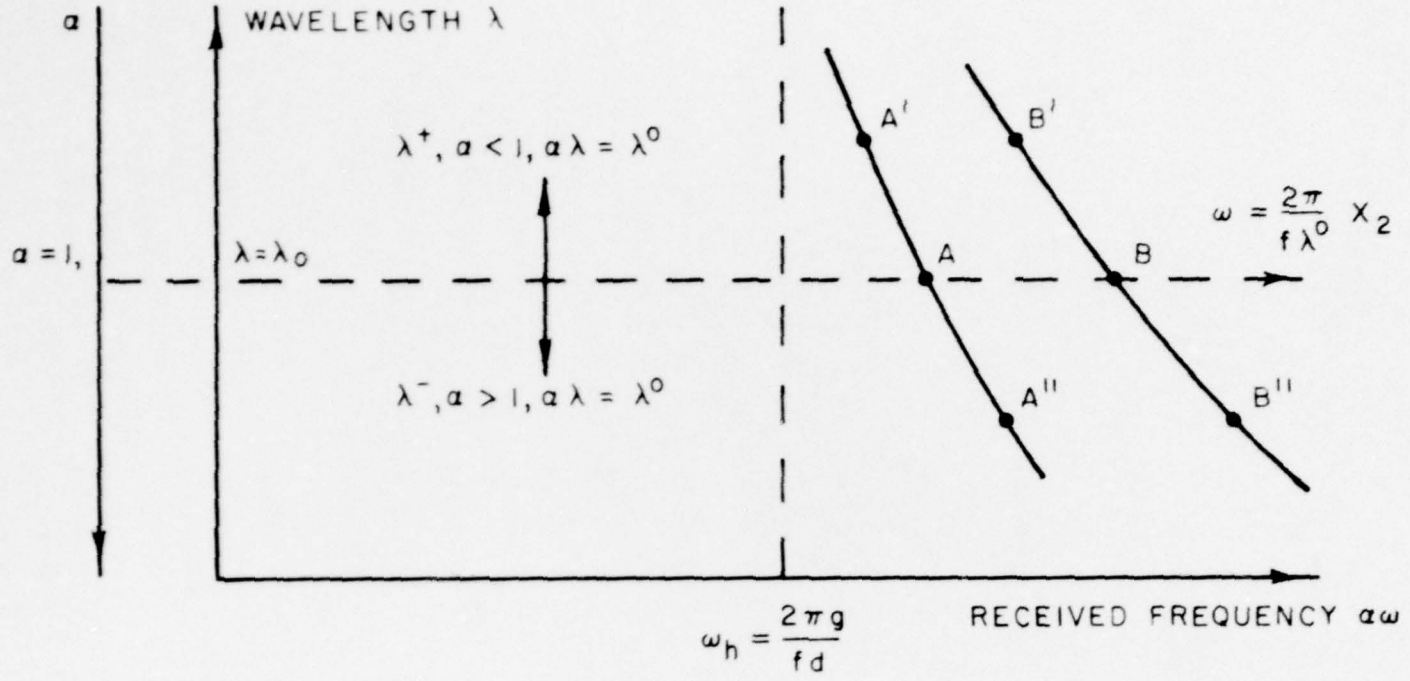

FIGURE 5 DOPPLER COMPENSATION IN PANCHROMATIC CORRELATION

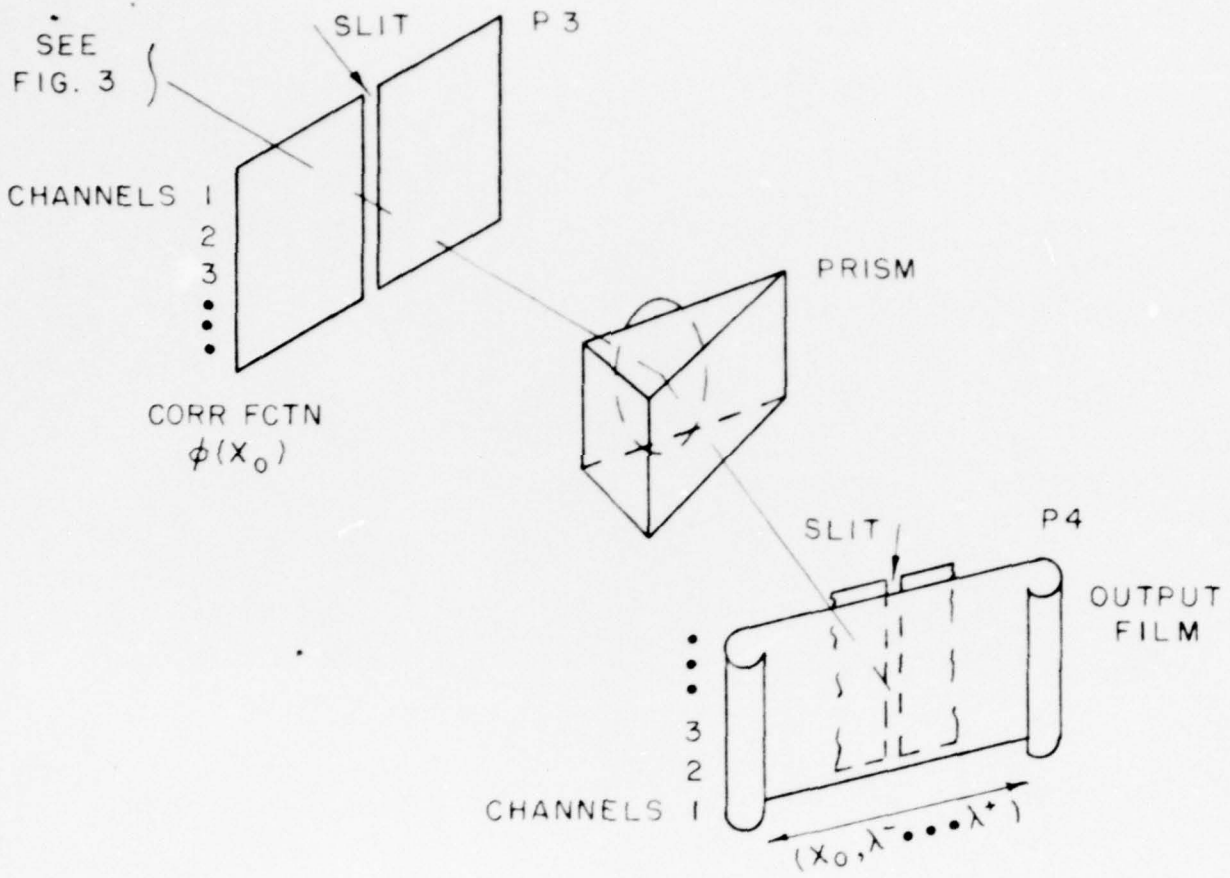

FIGURE 6 ALTERNATE CONFIGURATION, x_0 AND λ MULTIPLEXED

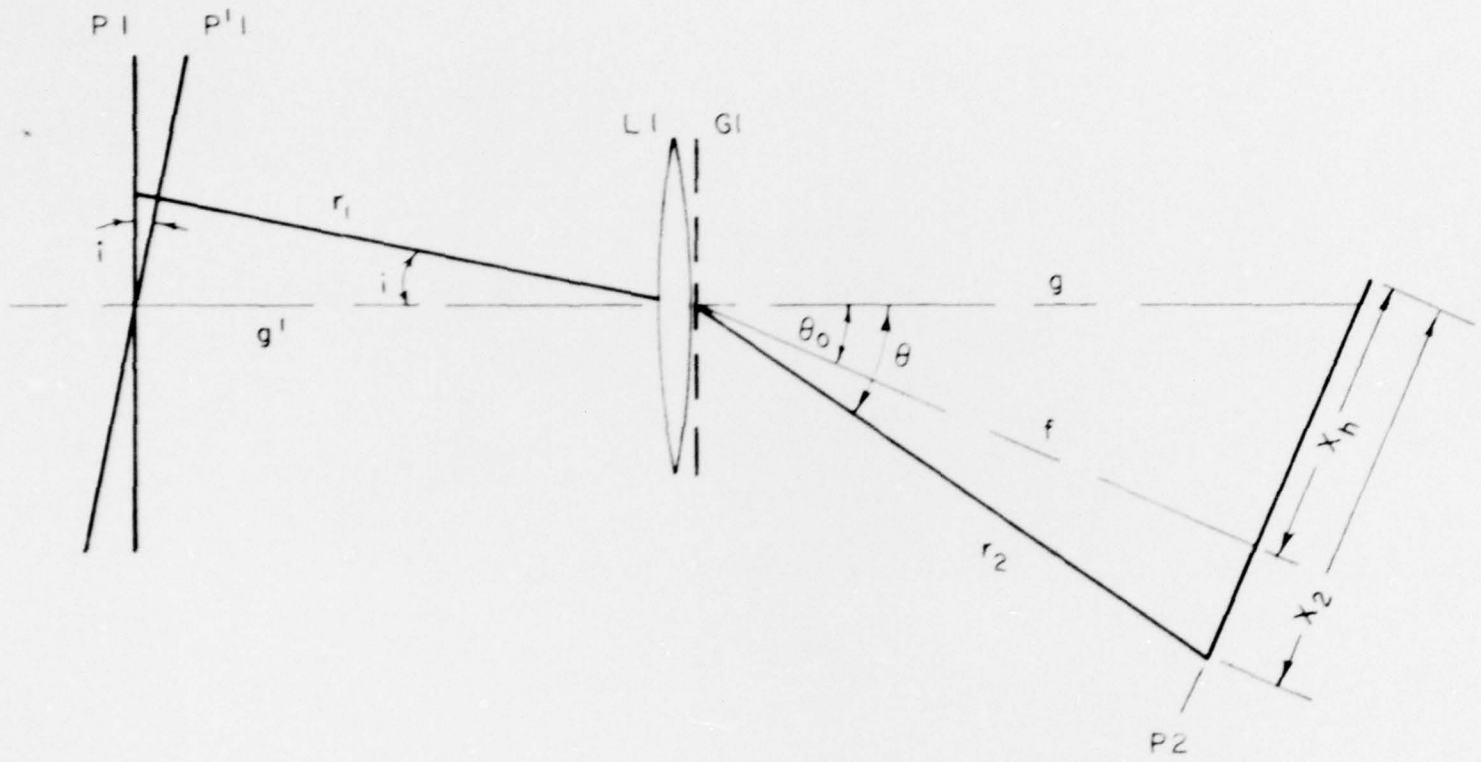

FIGURE 7 RAY PATHS IN $n = -1$ DIFFRACTION IMAGE